



# Observation of the Transit of Extrasolar Planet XO-2b

---

By

Alex Brockett, Ryan Phillips, Cory Stinson, Rhiannon Griffin, Fengming He

Department of Physics

UNIVERSITY of NORTH TEXAS

June 2009

## **Abstract**

The existence of planets outside our solar system is a topic that has long been debated but only recently (late 20<sup>th</sup> century-present)<sup>[1]</sup> been studied. The first telescopes used to detect extrasolar planets (ESP's) were very large, requiring dedicated staff and facilities<sup>[1]</sup>. With current advances in detection technology, however discovery of ESP's is now within the realm of much smaller single man / small team operations. Using a eleven inch Schmidt Cassigrain Reflector Telescope (SCRT), we were able to track and confirm the transit of a previously documented extrasolar planet XO-2b in the constellation Lynx. Observation occurred on February 6<sup>th</sup>-7<sup>th</sup> 2009 . The transit event lasted two hours forty-one minutes. Our results (13.4 mmag) showed that small scale telescopes are capable of clearly registering millimagnitude changes in the flux of variable stars during extrasolar planetary transits, and can be used to track, confirm, and even discover new extrasolar planets.

## **1. Introduction**

Extra-solar planet detection is a current interest in the astronomy community. The ultimate goal is twofold. One goal is to study solar system formation outside of our own <sup>[2]</sup>; another is to seek out habitable planets that may potentially support life <sup>[3]</sup>. To date there have been 360 confirmed discoveries of extrasolar planets <sup>[4]</sup>. However, due to limitations of the current observational technologies, most of the discovered extrasolar planets are gas giants, similar to Jupiter <sup>[5]</sup>. Also, due to technical variations in data, new discoveries often require verification by other institutions.

We, The Monroe Team, at the University of North Texas Monroe Robotic Observatory have photographed and analyzed the transit of XO-2b, and have obtained positive results. This success indicates that observation of an extrasolar planetary transit event is possible with the equipment of the UNT Monroe observatory.



There are several indirect methods for detecting extrasolar planets. These methods include: 1) the Doppler method, 2) the Transit method, 3) the Gravitational Microlensing method, 4) the Astrometric method and 5) the direct detection method <sup>[6]</sup>.

We have used the transit method for our experiment, which only required a moderate-size telescope and a sensitive CCD camera. The theory behind transit detection is simple, much like eclipse detection <sup>[7]</sup>. As a distant extrasolar planet crosses the line of sight between its star and Earth, high resolution telescopes can spot the slight dimming of the star's apparent brightness due to occlusion by the planet. Thus, a so-called light-well is formed on the star's light curve. In theory, the light-well should be symmetric. The best transit light curves allow modeling of the planet's basic properties such as mass, radius and distance from its parent star <sup>[8]</sup>. A non-symmetric light-well could indicate either an observational error or an abnormal transit. With the stated conditions, it is obvious that the transit method can only be viable for those extrasolar planets whose orbital planes intersect Earth; otherwise we could never see the transit. While other methods are more accurate <sup>[9]</sup>, the Transit method requires the least amount of sophisticated equipment.

## **2. Observations and Data Reduction**

The Monroe team observed XO-2b, a known extrasolar planet <sup>[10]</sup>. We received the ephemeris files from A. Shporer, 2008, private communication. Our observation occurred for two hours and forty-one minutes with one-hundred and sixteen images

being taken. Each image was taken with an exposure time of one-hundred and twenty seconds.

The equipment used in our observation consisted of a Celestron C11 telescope mounted on a German Equatorial Mount. In addition, we used a SBIG-XME CCD camera for our images. Basic photometry was performed and individual sets of compensation frames known as bias frames (BF), dark frames (DF), flat field frames (FF), and flat dark frames (FD) were created, in addition to the set of XO-2b images. The Bias frames measure the internal electrical noise of the CCD camera. They should be taken with a closed shutter for the least amount of time possible. The Data frames measure internal thermal noise of the CCD camera. It should be taken with an open shutter towards a dark plate for the same exposure time used for each image frame. The Flat field frames measure internal light reflections of the telescope as well as any reflections or refractions due to foreign objects on the telescope's optics. It should be taken towards a uniform light source that fills half the intensity capacity of the CCD camera. Lastly, the Flat Data frames are dark frames specifically designed for the Flat Field frames, taken with the same exposure time as the Flat Fields. The sets of BFs, DFs, and FDs are then median combined to produce Master BF (MBF), Master DF (MDF), and Master FD (MFD) frames. Then, a Master FF (MFF) frame is obtained from a normalized median combine of the Flat Field frames after subtracting the MBF and MFD from each Flat Field frame. The final calibrated image frames (CIF) are obtained from the raw image frames (RIF) by  $CIF = (RIF - MBF - MDF) / MFF$ , for each individual frame. The CIF set can then be plotted against the Julian date and analyzed for the modeling of the light curve.

## Subsection 2.1 **Observational Setup**

The Monroe Robotic Observatory (MRO) is a UNT-owned observatory located near Gainesville, TX. It will consist of five telescopes, and currently includes the 11-inch telescope used for the planetary transit observation. The MRO's coordinates are Lat.  $33^{\circ} 46' 36'' \text{ N}$  and Long.  $97^{\circ} 12' 39'' \text{ W}$  at an elevation of 707 feet (215.49 m)<sup>[11]</sup>. It is a

remote site with minimal light pollution. The observatory is remotely controlled from the UNT Denton campus, including the roll-off retractable roof. Although the observatory can be accessed on site, most observations are conducted from its control center in room 363 of the Environmental Education, Science and Technology building.

The Celestron C11 SCT telescope used for the observations has an aperture of 279 mm, and the focal length is 55.1 inches (1400 mm) <sup>[12]</sup>. An Optec Focal Reducer was added to the telescope to give it a focal length of 110.2 inches (2800 mm). Images were collected with the Kodak based SBIG ST8-XME imaging camera. The pixel size is 9  $\mu\text{m}$  square with each having a field of view around 0.7 arc seconds, and the pixel array is 1530  $\times$  1020. This gives a total of 1.6 million pixels. This CCD measures out A/D gain of 2.3 e<sup>-</sup>/ADU and a read noise of 11.09 e<sup>-</sup> RMS (on-chip noise) <sup>[13]</sup>. Along with the CCD, an Optec TCF-S Temperature Compensated Focusing system and Optec IFW Filter Wheel system (with U, B, V, R, I filter set and wheel assembly) are used for the image collection. To guide the telescope a f1.39 guide scope is used with a SBIG ST5C imaging camera. The Celestron C11 sits on a Paramount ME German Equatorial Telescope Mount. Software used includes Maxim DL v4.61 for imaging the transit, Mira v7.966UE for image reduction, and The Sky v6.0.0.53 for comparison star information <sup>[14]</sup>.

## Subsection 2.2 Observing Conditions

The observations for the XO-2b transit were conducted between 10pm on 2009 February 6<sup>th</sup> to 2am on February 7<sup>th</sup> CST (Universal Time – 6). The weather data is collected and graphed in UTC. This weather data must be taken into account when we examine the raw data, as cloud cover became a problem at the end of the observation. Fig. 1 shows three diagrams displaying the total cloud cover <sup>[15]</sup> over three hour periods during the observation. The star on the diagrams represents the location of the MRO. Atmospheric moisture and humidity are also very important to monitor along with cloud cover. To limit the effects of atmospheric moisture, the observation of the planetary transit was calculated to be collected with the lowest airmass possible, when it is directly overhead. Therefore the middle of the transit should occur overhead. Humidity

can also become a problem with the telescope. The humidity can cause dew to form on the corrector lens of the telescope or on the exteriors of the CCD. Both of these can add significant noise to the images. The second graph of weather data <sup>[15]</sup> displays the temperature and the dew point for the same time frame, and this shows that dew should not have been a problem for the time of the observation.

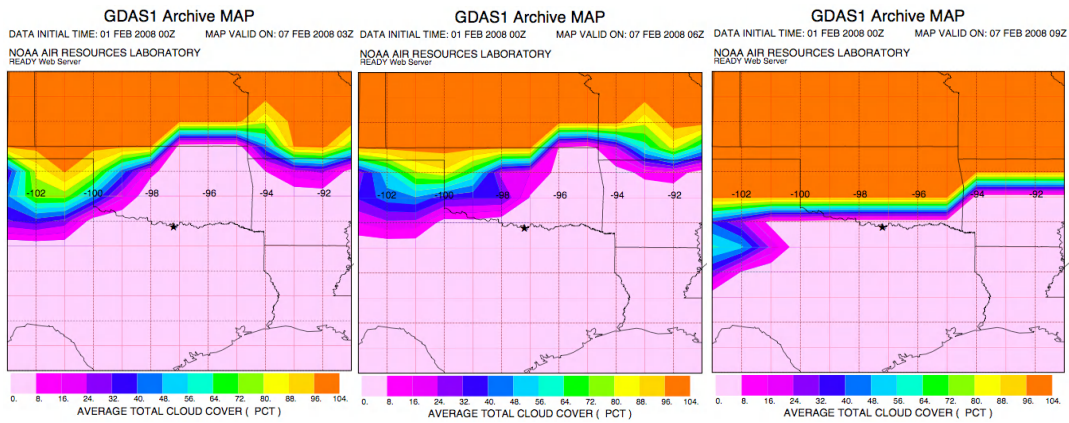


**Figure 1.** Cloud Cover for Monroe Robotic Observatory during observations. <sup>[15]</sup>

# NAM12 Archive METEOROGRAM

Latitude: 33.78 Longitude: -97.20

DATA INITIAL TIME: 07 FEB 2009 00Z  
 NOAA AIR RESOURCES LABORATORY  
 READY Web Server

CALCULATION STARTED AT: 07 FEB 2009 00Z  
 CALCULATION ENDED AT: 07 FEB 2009 06Z

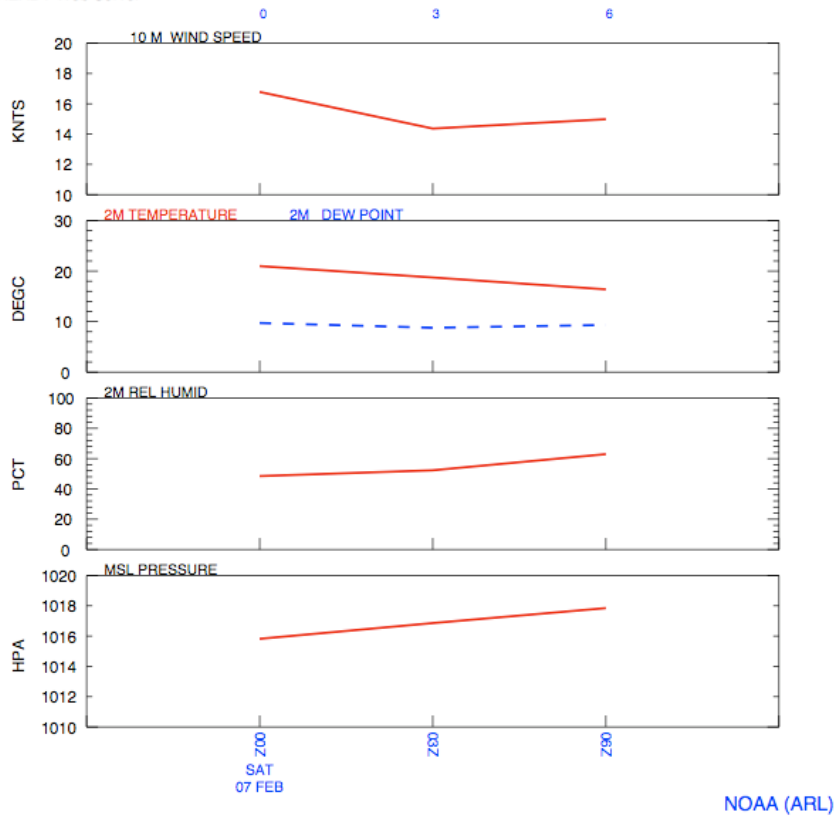


Figure 2. Weather data at the Monroe Robotic Observatory during observations. <sup>[15]</sup>

## Subsection 2.3 Creating Calibration Frames for the data images

The data taken from the X0-2b transit event was processed and analyzed using the photometry program MIRA 7UE (ultimate edition). A V filter was used for the observation. The following procedure was conducted to obtain the data for our statistics based on recommendations from Ron McDaniel, the Monroe Team’s Mira expert.

1. First, in order to obtain a clean image with a high signal to noise ratio the electronic noise produced by our CCD camera must be subtracted from all of our raw data images and other calibration images. This electronic noise is known as the Bias.

The Bias frames are taken at the same temperature at which the data images were taken by our CCD camera. Each frame is exposed for the minimal time possible. There should be no light entering into the camera during these exposures. For our image set we took a total of twenty-five Bias frames

In our version of MIRA, the Bias frames are combined by opening all the frames into one set of images. The images are a 32bit-real data type and the combine method is median value. Using the median values of each pixel value range, we disregard the highest and lowest values, and take only the middle values. This will expel any abnormalities. Once the Bias frames have been combined they are to be saved.

2. Now that we have our MasterBF we need to subtract its pixel z-values—the depth of the light well—from our Dark Data frames. Data frames are calibration frames that compensate for thermal noise generated by the CCD sensors. The frames were taken with the same exposure time as our image frames and at the same temperature with which our camera was operating during the transit imaging.

In order to isolate the thermal noise in our Data frames, we must subtract the MasterBF from our Data Frames. This is accomplished in one of two ways. One method is the MasterBF is express calibrated to each Data Frame individually and then the resulting frames are combined using a median combination method. The second method is the Data Frames are combined first and then the MasterBF is applied to the resulting single Data Frame. The frame is then named as our MasterDark.fts. The second method produced a frame that had a smaller z-value range than the frame calibrated using the first method. The z-value range for the second frame was approximately one half of the first frame. When calibrating the image frames the second MasterDF with the smaller z value range was used.

3. The next set of calibration frames are the Flat Field Dark Frames. These frames also account for thermal noise associated with the CCD's sensors. The frames are

taken with an exposure time that equals the amount of time for the filter to fill one half of its full well capacity for the camera in a uniformly lit area. The Flat Field Dark frames are taken with no light.

As with the other calibration frames, the MasterBF must also be subtracted from the Flat Field Dark frames. Both of the same methods used for creating the Master Dark frame were used in creating the MasterFFD. The frames created from the first and second methods had negligible differences in their z-value ranges. The first frame was used to calibrate the data images. This frame was named MasterFFDark.fts.

4. The final calibration frames to be prepared are the Flat Field frames. Flat fields account for physical objects on the lens of the camera and internal reflections due to the telescopes mirror and lens. The frames also account for any foreign objects on the mirror and lens.

Preparing the Flat Field frames differs from the previous calibration images in that we must also subtract out the MasterFFDark frame as well as the MasterBF. The Flat Field frames must be combined by normalizing the pixel z-value and scaling the results to one. Our Flat Field frames were non-uniformly lit which contributed as error in our final results.

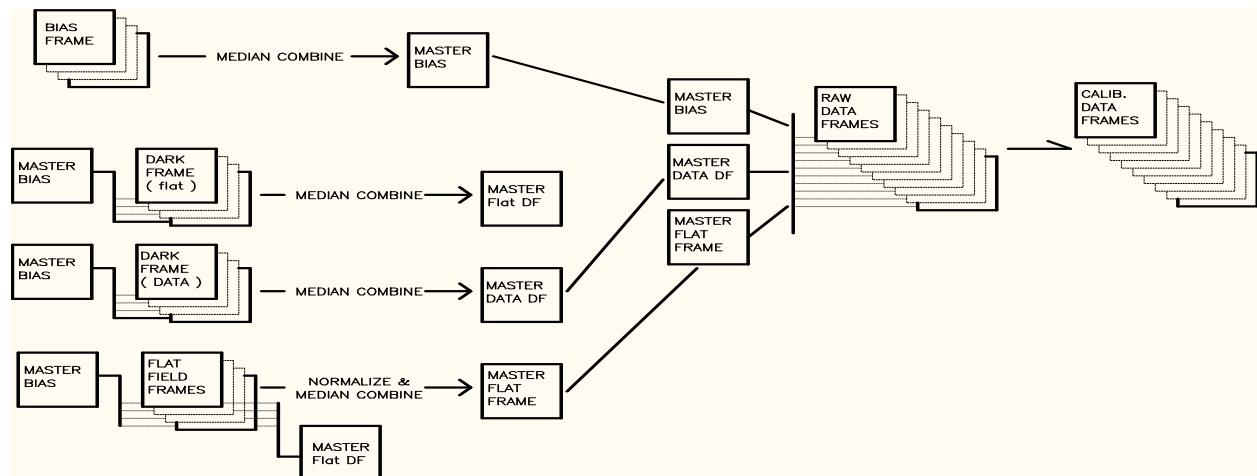


Figure 3. Calibration Procedure Flow Chart. [16]

## Subsection 2.4 Spatially Calibrating the Images for Photometry

Two separate sets of images were taken during observation because a meridian flip had to be performed during the transit event. Due to the physical limitations of a German Equatorial Mount, the telescope may only have a continuous viewing field in one direction from the horizon to the observer's meridian before it must be rotated to view the second half of the sky; this is called a "meridian flip". Before the calibration of the images could be accomplished, all of the frames had to be matched in position. This was done by opening the first set of images that were taken before the telescope meridian flip into the first set. Next, the set of images taken after the meridian flip is opened into its own set. Once both sets are open, take one set and rotate it 180° to compensate for the meridian flip. One set should be rotated to match the other.

## Subsection 2.5 Photometry

Now that the images have been matched they must be synced to a stationary point. As the telescope tracked the target XO-2b, the guiding system was slightly displaced from the object and drifted further away from XO-2b over time. This common error must be accounted for by registering the images.

When registering the images, we first picked four or five stars to track through the image sets. When picking the four to five tracking stars we chose stars that were clearly visible and isolated. One of these stars was XO-2. Once the stars were chosen they were tracked, calculated and applied. The Tracking function process takes each of the chosen stars and selects the same stars throughout the image sets. The Calculating function measures the distance each star must move in each frame to remain stationary. The Applying function applies those corrections through the entire image set. When we completed the registering process we viewed the images in sequential order. After applying these operations to both sets of data we began the photometry portion of the reduction.

For this process we had chosen a total of four check stars and one comparison star. Comparison star is a star with known magnitude. It is used to judge the magnitude

of the variable star. The check stars are noise indicators and judge whether or not the comparison star is a variable star. When these stars were marked, their magnitudes were entered and names were assigned. The magnitudes were acquired from the Sky6 v.6.0.0.53 program [14]. Once the apertures are set on the stars they can be adjusted to gain a larger signal to noise ratio. We used the program's default automatic aperture adjustment function for our data sets. The last step is to use the calculate function to complete the reduction of the data. After the calculation there will be three columns which contain the Julian dates, instrumental magnitudes and errors. Next is the statistical analysis of the reduced data.

### 3. Results

The photometric data output from MIRA was used to plot a light curve. Figure 4 shows the light curve plotted with error bars. The light curve shows the magnitude of the star over time (in JD-2453000). Figure 4 clearly shows the dip in the light curve.

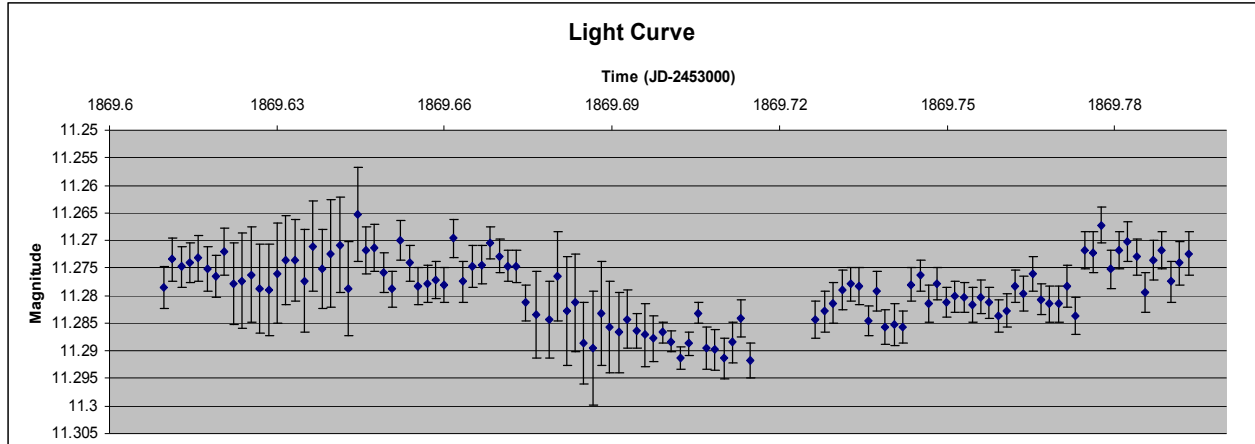


**Figure 4.** Light curve of XO-2 with error bars

Note the gap in the light curve from  $x = 1869.714664$  to  $x = 1869.726412$ . This gap of about seventeen minutes is when the telescope performed a meridian flip and no pictures were taken. Also, note the change in the size of the error bars from the last half of the curve when compared to the first half of the curve. Possible reasons for this are discussed in Error Analysis.

To test whether the light flux from XO-2 is variable, we used two variations of the  $\chi^2$  test. The  $\chi^2$  test compares a null hypothesis to an alternative hypothesis and gives a P value statistic. The P value is the probability that random points would cause the amount of discrepancy between the observed values and the expected values, assuming the null hypothesis is true. If the P value is sufficiently small, the null hypothesis is rejected and other hypotheses need to be considered. A null hypothesis with a P value that is less than one percent is considered to be statistically significant and a null hypothesis with a P value that is more than one percent is considered to be highly statistically insignificant. To get the  $\chi^2$  test statistic, use the following function:

$$\chi^2 = \sum_{i=1}^n ((O_i - E_i) / \sigma_i)^2$$

where  $n$  is the number of data points,  $O_i$  is the set of observed quantities,  $E_i$  is the set of expected quantities, and  $\sigma_i$  is the set of errors. The degrees of freedom are the number of parameters minus one, so in this case  $n - 1$ . Using the  $\chi^2$  test statistic and the degrees of freedom, one can get the P value.

First, to check if XO-2 is a variable star, we assumed a null hypothesis that it is non-variable. To compute the  $\chi^2$  test statistic, we compared the observed data points with a constant expected value of 11.2748. This is illustrated in Figure 5. The expected value was found by taking the average of the first forty-two data points, since this was the magnitude of the star before the transit event. This gave a  $\chi^2$  test statistic of 529.8893 and a P value less than  $10^{-4}$ . This implies that the null hypothesis can be rejected. This does not imply that this event is an extrasolar planet transit, just that XO-2 is a variable star.

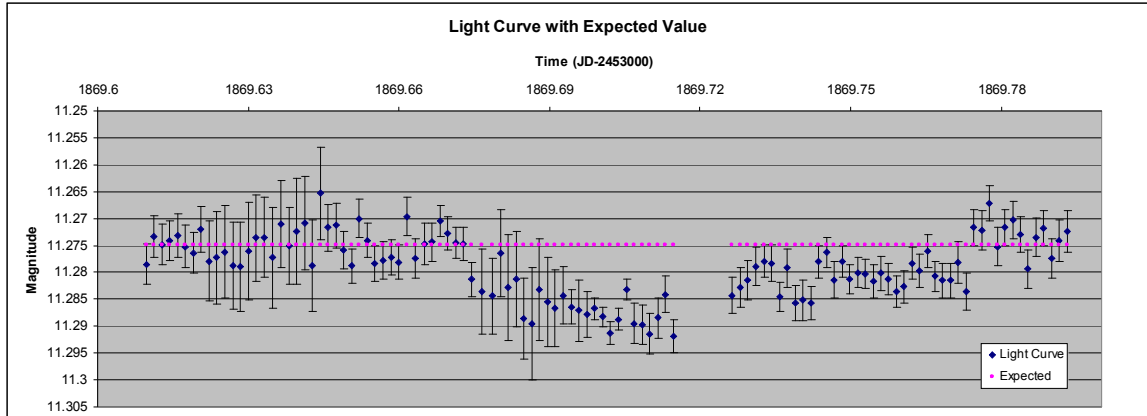


**Figure 5.** Light Curve with the expected value of the curve if XO-2 was not variable

Next, we fitted the best model to the light curve. A standard light curve of a star with an extrasolar planet consists of three main components: a constant line before and after the event, a constant line in the middle of the event, and a sloping line as the planet begins and ends the transit. These three main components make up the dip that characterizes a planet transit. There are other more complex models, but given the quality of our data it can only warrant a simple “trapeze” model. For the fitting, we used data before the meridian flip, which occurred from 1869.714664 to 1869.726412. The dip in the light curve is assumed to be symmetric so a best fit line for the first half can be flipped to fit the second half as well. Figure 6 shows the light curve with the best fit line. The first component is the constant line at magnitude 11.2748 mags the magnitude measured just before the event. This gave a  $\chi^2$  test statistic of 22.3715 and a P value of 0.9921. The second component is the constant line at 11.2882 mags, the magnitude measured from the star while the planet is transiting. This gave a  $\chi^2$  test statistic of 13.9317 and a P value of 0.3787. The third component is the line:

$$y = 0.2785x - 509.5$$

where  $y$  is the magnitude and  $x$  is the time in Julian Date – 2453000. We fitted this model using the  $\chi^2$  distribution to test for goodness of fit<sup>[17]</sup>. We found the best fit line using the eleven data points starting from  $x = 1869.676458$  to  $x = 1869.692743$ . This gave a  $\chi^2$  test statistic of

1.592649 and P value of 0.9986. This was the highest P value found, even when changing the amount of data points and the best fit line through the data points. These best fit lines were found for the first half of the curve and flipped to fit the second half of the curve, since this is what is expected for a smooth light curve. However, the second half of the light curve does not fit the previously found best fit line. See Subsection 3.1 for possible reasons for this discrepancy.

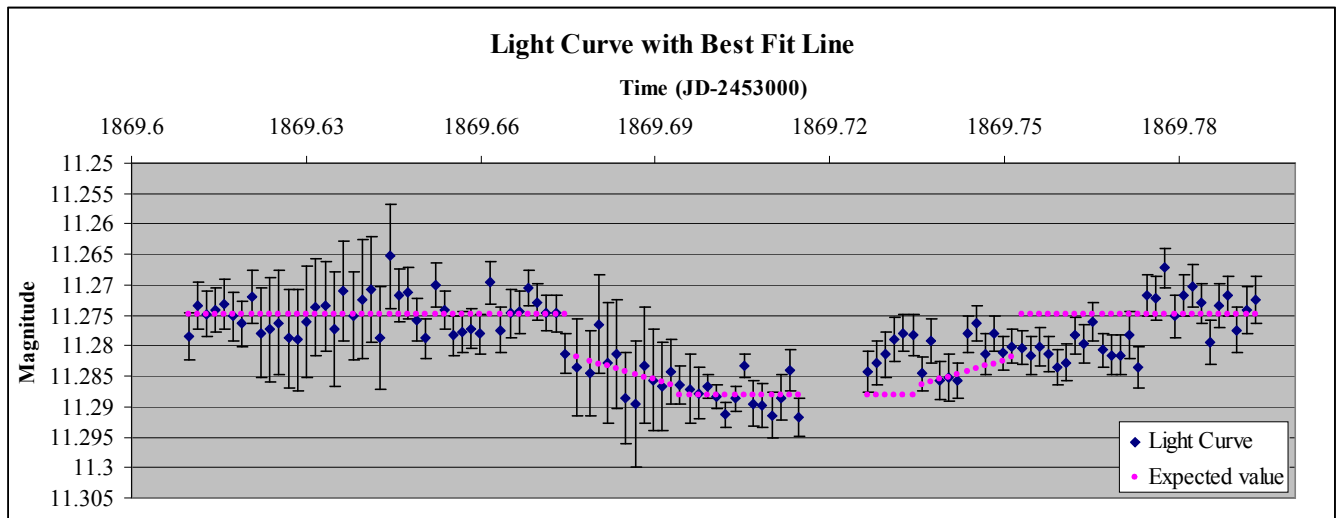


Figure 6. Light Curve with the best fit model

### Subsection 3.1 **Sources of Error**

The following sources of error were considered in the analysis:

1) Cloud cover during last 30 minutes of post transit observing caused a large fluctuation in magnitude during gathering of base line data. This may explain why the best fit line for the first half of the curve does not fit the second.

2) Position of the telescope for flat field frames was slightly skewed causing a gradient to form in the frames. This does not allow the flat field frames to fully compensate for dust and irregularities in the lens or internal reflections within the mirror assembly of the telescope.

3) There is the inherent error associated with the meridian flip during the middle of the transit which left a seventeen minute gap in the middle of the transit.

4) There were also errors associated with the various processes performed by the MIRA software. Each of the noise reduction sets is median combined leaving out the highest and lowest values. This reduces noise but cannot eliminate it. During the actual process of photometry, the two annuli and target rings can be altered also eliminating noise but at the cost of reduced signal.

### 4. **Conclusions**

Using an eleven inch telescope, we were able to detect a transit event of XO-2b. The transit lasted two hours and forty-one minutes with a dip magnitude of 13.4 mmags, which confirms the variable star XO-2 to be harboring an extrasolar planet.

This is another confirmation that relatively small telescopes are sufficient for tracking and discovering extrasolar planetary transits.

## **Acknowledgments**

The Monroe Team would like to thank the following people:

Ron McDaniel, for the use of his equipment, software expertise, and years of experience in astrophotography. Ron “Starman” Dilulio and Preston Starr, for their technical expertise. Dr. Ohad Shemmer, for guidance

## **References**

- [1] Wolszczan, A.; Frail, D. A. (1992). "[A planetary system around the millisecond pulsar PSR1257+12](#)". *Nature* **355**: 145 – 147.
- [2] <http://www.nature.com/nature/journal/v460/n7259/full/nature08245.html>
- [3] <http://bostonclub.mit.edu/news/46-bss/172-boston-seminar-series-begins-with-extrasolar-planets-and-the-search-for-habitable-worlds-on-917>
- [4] <http://planetquest.jpl.nasa.gov/>
- [5] [http://www.adlerplanetarium.org/cyberspace/Explorers/Out\\_There/Extrasolar\\_Planets/](http://www.adlerplanetarium.org/cyberspace/Explorers/Out_There/Extrasolar_Planets/)
- [6] [http://planetquest.jpl.nasa.gov/science/finding\\_planets.cfm](http://planetquest.jpl.nasa.gov/science/finding_planets.cfm)
- [7] <ftp://ftp.iac.es/tepstuff/puerto97/transitmet.pdf>
- [8] <http://adsabs.harvard.edu/abs/2009ApJ...693..794W>
- [9] <http://arxiv.org/abs/astro-ph/0603005>
- [10] <http://adsabs.harvard.edu/abs/2007arXiv0705.0003B>
- [11] [www.earth.google.com](http://www.earth.google.com)
- [12] <http://www.celestron.com/c3/product.php?ProdID=87&CatID=15>
- [13] <http://www.sbig.com/sbwhtmls/ST8XME.htm>
- [14] The Sky6 v6.0.0.53, Software Bisque
- [15] <http://www.srh.noaa.gov/ffc/html/archives.shtml>

[16] Ron McDaniel personal presentation

[17] <http://www.itl.nist.gov/div898/handbook/eda/section3/eda35f.htm>